# Geostatystical approach to spatial, multi-elemental dataset from an archaeological site in Vatnsfjörður, Iceland

Łukasz Mikołajczyk and Karen Milek, University of Aberdeen.

## 1. Introduction

Understanding the spatial patterning of human activity is of crucial importance to the interpretation of any archaeological site. Not every site has a well-defined stratigraphy, or a material record, that can be used to grant insight into the nature of the activities that were undertaken, and how these were distributed. In such cases, geochemistry can provide a cheap and effective solution for characterising the use of archaeological space. The core principle behind archaeological geochemistry is that human activity causes chemical distortion (enrichment or depletion) to the local substrate (Oonk et al. 2009, Middleton et al. 2010 with references ). This chemical signal can be used to 'fingerprint' the types of activities that were taking place. There are, however, limitations to the method linked to difficulties in differentiating the origin of the chemical signal (Oonk et al. 2009). For example, problems arise when attempting to identify multiple deposition episodes, through the possible influence of diagenetic processes in altering the chemical signal (Middleton et al. 2010), and as a consequence of the statistical methods used to process multivariate datasets (Entwistle et al. 2007; Dore and Lopez Varela 2010). In this paper we highlight this problem and tackle it though the application of the methodological framework proposed by Dore and Lopez Varela (2010) with some modifications. Rather than using only a limited suite of soil-chemical measurements (i.e. phosphates, carbonates, pH, protein residues, and fatty acids), we adopt an approach in which a multi-elemental dataset is produced and analysed. In doing so we highlight the statistical procedures that we consider to be the most crucial for an informed interpretation of human activity at an archaeolgical site, using a farm in Iceland as our reference case. At this location, the interplay between human pressure and natural processes (e.g. relative sea level change) was considered important in influencing the pattern and character of activity, and therefore a method for establishing a wide range of elements was used (X-ray fluorescence). In such a situation, not only is the anthropogenic signal able to be studied, but also the natural processes affecting the site can be taken into consideration (Linderholm and Lundberg 1994).

Geochemical studies of coastal archaeological sites are not unusual (see Knudson 2004; Ilves and Darmark 2011 with references; Misarti et al. 2011). There are several studies of this type in Iceland; most have used phosphate (P) analysis (Bolender, 2003; 2006; Simpson et al., 2002; Mikolajczyk et al. 2015), and there is one multi-elemental study (Milek and Roberts 2013). This paper builds on previous research in this field through the application of archaeological geochemistry to the iron- and allophone-rich andosols that are specific to Iceland (Arnalds et al., 1995; Arnalds, 2004).

## 2. Study area

The farm of Vatnsfjörður is located in the Vatnsfjörður fjord, northwest Iceland, and has been continuously occupied from the 10$^{th}$ century AD to the present day. Written sources mention Vatnsfjörður as one of the original *landnám* farms that in the 12$^{th}$ and 13$^{th}$ centuries served as a Chieftain’s seat. It was also the location of a church reputed to be the second wealthiest on the island. The site kept its priviliged position until the end of 16$^{th}$ century. The site consists of three components (Fig. 1, left): the Viking-age settlement area, the Medieval to Early-Modern farm mound, and an extensive coastal zone (Milek 2011: 17-22). The coastline in the Vatnsfjörður area is not stable. Glacio-isostatic crustal movement and glacio-eustatic sea-level rise are responsible for relative sea-level (RSL) changes in the area. RSL was at least 1 m greater than at present during the mid-Holocene, subsequently gradually falling to the present-day level (Norðdahl and Pétursson 2005; Lloyd and Dickens 2011; Mikolajczyk et al. 2015).

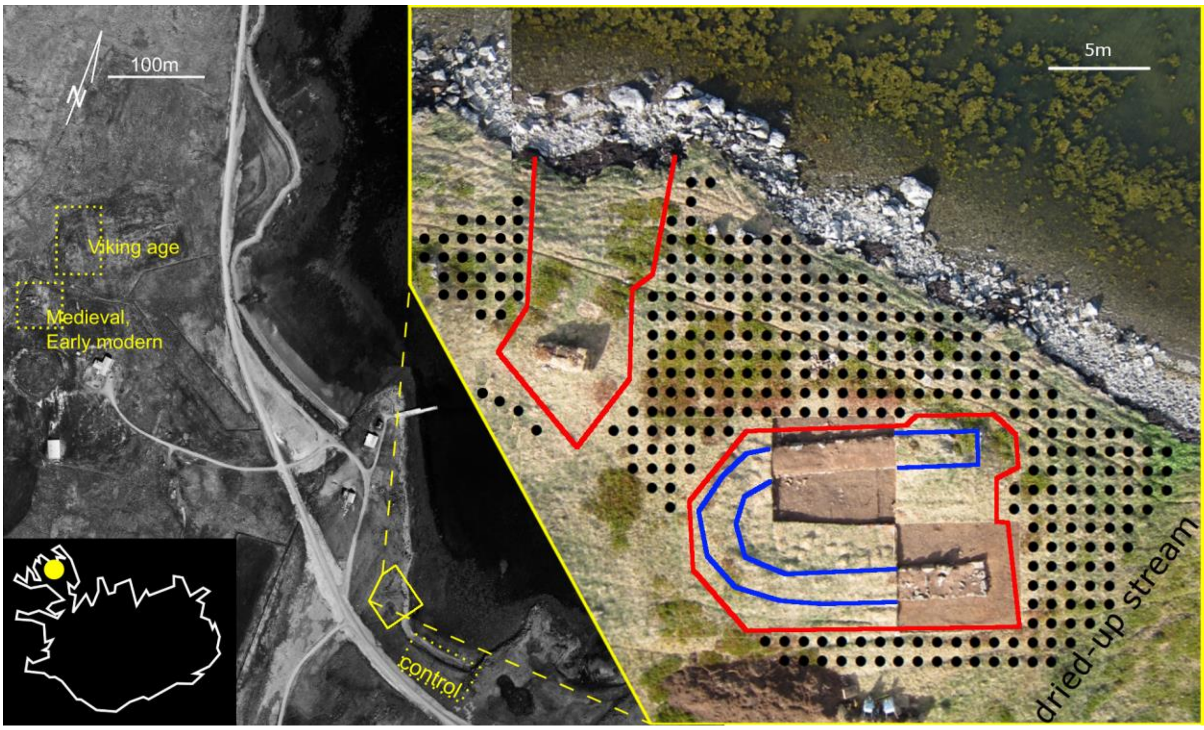


Fig. 1. The archaeological site of Vatnsfjörður: Left, aerial photography of the site. Visible are the Viking age, Medieval and Early-Modern settlements plus the coastal zone, studied excerpt and control sampling area. Right, enlarged studied section of the coastal zone. Visible, in red, are the extents of v-shaped (left) and u-shaped (right) structures’ collapsed material; in blue, structural walls; in black, the location of sampling points.

The archaeological coastal zone at Vatnsfjörður stretches c. 1500 m along the shoreline and consists of three pronounced subzones, all of which still bear visible traces of intensive use in the past (Fig. 1). All three were targeted with small scale archaeological investigations (Mikołajczyk and Gardeła 2010: 48; Mooney et al. 2012: 49-50; Mooney 2013: 40-48, Mikołajczyk 2013) and phosphorous (P) transect mapping (Mikolajczyk et al. 2015). The most complex situation was encountered in Zone B where at least two, not necessarily chronologically-discrete phases of activity of unknown intensity merge in a relatively small area. Henceforth results were deemed insufficient to understand the character of human occupation in this area and for this reason extensive multi-elemental mapping of the area was employed, the results of which are presented in this paper. Zone B is located at the southernmost edge of Vatnsfjörður and is dominated by the ruin of a massive, 15 m long, U-shaped building (Fig. 1B) (Mikołajczyk and Gardeła 2010: 48). It has been excavated (Mooney et al. 2012: 49-50, Mooney 2013: 40-48), but despite the detailed information on its construction method – the building is characterised by a very robust, 1.5 m thick, stone-lined, turf wall – its function remains unknown. It yielded neither datable material nor any other finds, and its internal floor layer is very thin and non-diagnostic (Mikołajczyk 2013). The shape of the building is similar to boathouse constructions. Results of the P mapping (Mikołajczyk et al. 2015) revealed an unusual orientation, parallel to the modern shoreline, facing the embayment at times when sea level was higher. The aforementioned research managed to date the activity area in front of this structure to the late 15$^{th}$ century on the basis of its elevation relative to sea level at this that time; this agrees with the general *ante quem* date for human activity in the zone that is stratigraphically below the tephra from eruption of Hekla dated to AD 1693. There are also three other ruins in the northern part of zone B, all of which are in a rather poor state of preservation (Fig. 1B). Two of them are c. 6 m long, V-shaped, overlapping boathouse-like structures and the third is a small, rectangular, stone-lined structure with walls abutting a natural bedrock outcrop. The activity area immediately east of the V-shaped structures was dated to late 12$^{th}$ century. The age of the rectangular structure is unknown. In the area to the west of the V-shaped structure, a slight depression in the terrain was noticed. A test trench placed there yielded some burnt seaweed fragments.

## 3. Methods

### 3.1. Sampling

316 soil samples were taken from 0.2x0.2 m shovel test pits placed according to a 1x1 m grid fixed on cardinal directions. Grid points were recorded with the use of a Trimble DGPS unit, with 1 cm accuracy. Special care was taken to sample soil strata recognised as corresponding to the archaeological structures. However, due to the thinness of the soil and the patchiness of the only chronological marker on the site (the H-1693 tephra layer), in some cases, samples had to be taken at an arbitrary depth of 0.05 m below the dense grass root mat (as that was the average depth of the H-1693 tephra when present). Additionally, a control group of 20 soil samples was taken in an opportunistic manner from two neighbouring areas without any visible archaeological features (Middleton and Price 1996).

### 3.2. Sample processing

336 samples, each weighing c. 20 g (dry), were oven dried, gently pulverized and subsequently analyzed using an Olympus-Innov-X Delta Premium XRF scanner stocked with Au anode tube. The device was operated in a 3 beam ‘soil’ calibration mode and in a desktop setup allowing for convenient long exposure times. Prior to the main analysis, reference material (soil samples with known elemental ratios) was tested multiple times in order to select the exposure time that provided best repeatability. Samples were analyzed for S, K, Ca, Ti, V, Mn, Fe, Cu, Zn, Br, Rb, Sr, Zr in the following set up: beam 1 - 40kV at 30s exposure time; Beam 2 – 40kV at 30s exposure time; Beam 3 – 15kV at 60s exposure time. All results are semi-quantitative.

## 4. Analysis

Due to the apparatus characteristics some P readings (c. 5%) yielded relatively high detection errors. In order to account for this, problematic readings were corrected with a use of values sub-sampled from the interpolation curve created on the base of the remaining dataset. Readings for Ca, Mn, Fe and Cu yielded few outliers that in order to maintain a more natural distribution of the data set were managed by winsorisation (Chambers et al. 2000). Before computation, the data were standardized to avoid scaling effects and to obtain average-centered distributions (Baxter 1995)

### 4.1 Spatial analysis

The spatial analysis was conducted using ArcGIS 10.2 (ESRI 2015) in a manner similar to that followed by Dore and Lopez Varela (2010). The readings at sampling points for separate elements were projected in a 2D space according to their x-y position on the site grid. Subsequently, respective surfaces were interpolated by ordinary kriging. When necessary, in order to account for potential directional influences, the second polynomial trend was removed and interpolation weights were adjusted for anisotropy, the aim being to obtain a model with the best cross-validation scores. Surfaces were subsequently turned into elemental raster layers with floating point pixel type in 32 bit color depth with pixel size of 0.1 m. (Fig. 2). The rasters were subjected to principal component analysis (Pearson 1901, Hotelling 1933). This procedure allows not only the ‘noise’ to be removed from the dataset, but it also eliminates redundancies caused by highly correlated variables (Table 1 ). With the use of the data fusion technique, this allows for efficient visual inspection of the spatial structure of variance (Craig et al. 2006; Devereux et al. 2008; Kvamme 2006, 2007; Richards and Jia 1999). The first three components that usually explain a gross part of variance were plotted as red, green and blue channels of a composite raster, presenting a multi-color representation of data spatial variability (Fig. 3.). Correlation coefficients of elemental and component rasters were calculated indicating elemental loadings for particular components (Fig. 4 and Table 2). Subsequently, elemental rasters were subjected to unsupervised classification using an iterative self-organizing (ISO) clustering algorithm and a Maximum

Likelihood Classification tool. Various numbers of determined classes were considered with the goal being to obtain a classification that is visually the most concordant with the principal component raster, and most meaningful with regards to the site's spatial variability. Finally, a seven class output was chosen (Fig. 5) and all sampling points were grouped according to the class affiliation (Fig. 6).

| Elements | | Correlation coefficient |
|---|---|---|
| Ti | V | 0.92 |
| Ca | Sr | 0.86 |
| K | Zr | 0.81 |
| Zn | Sr | 0.79 |
| Ca | Zn | 0.75 |
| Ca | Br | -0.74 |
| Ca | Mn | 0.71 |

Table 1: List of the most highly correlated elements ( correlation coefficient >0.7).

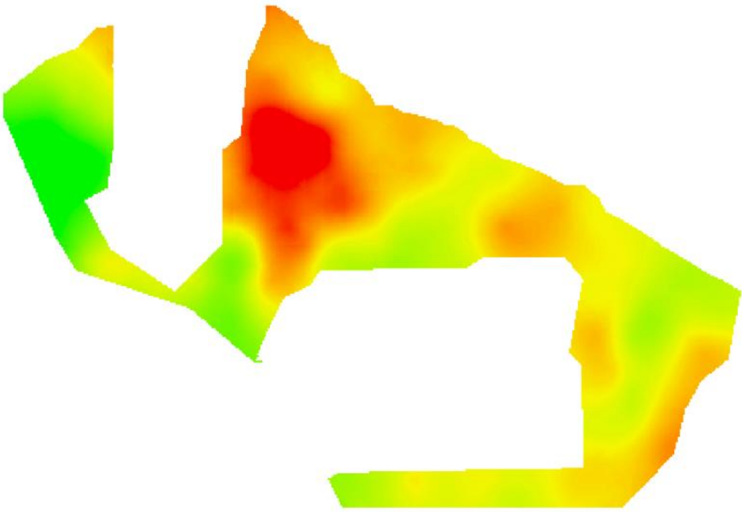

Fig. 2: An example of an interpolated elemental raster (for phosphorus) with values on the scale from low (green) to high (red).

4.2 Computational analysis

Further calculations were conducted on the raw data in using R software (R Core Team 2014). Class summary statistics were calculated and compared with the mean of on-site values. Deviations from the mean on two levels (>0.5 s.d. and >1.0 s.d.) were recorded (Table 3). Together with the PCA matrix (Fig. 4), these serve as a base for class interpretation.

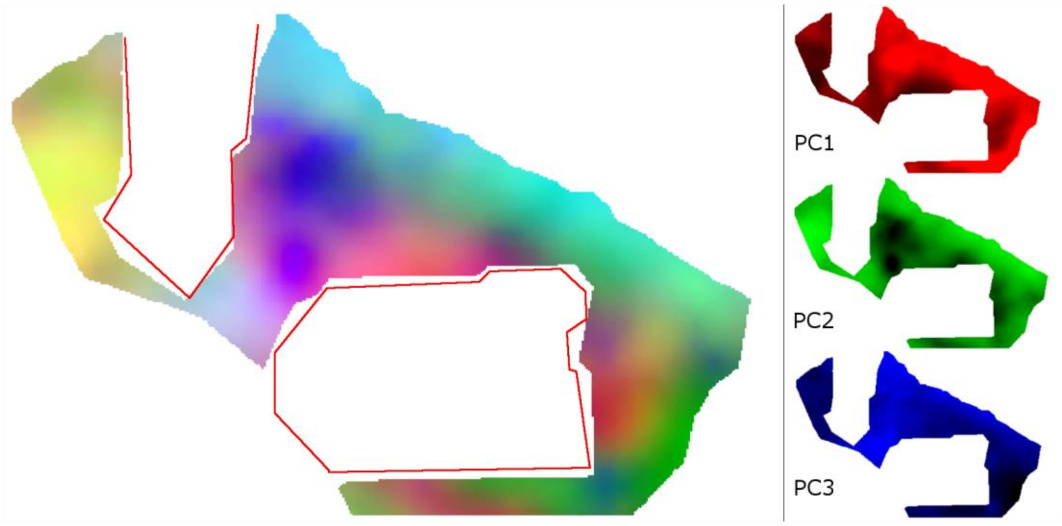


### 4.2.1 PCA results

Fig. 3: Spatial projection of the Principal Component Analysis (PCA) results. Right: spatial distribution of variance for separate components depicted in red, green and blue; positive loadings - lighter, negative loadings- darker. Left: data fusion, tree components projected jointly with the outlines of buildings depicted in red.

| Components | PC1 | PC2 | PC3 |
|---|---|---|---|
| P | 0.55 | -0.61 | 0.34 |
| S | -0.46 | -0.78 | 0.16 |
| K | 0.45 | 0.16 | 0.78 |
| Ca | 0.37 | 0.54 | -0.07 |
| Ti | 0.61 | -0.38 | 0.32 |
| V | 0.84 | -0.34 | -0.20 |

| | | | |
|---|---|---|---|
| Mn | 0.84 | -0.37 | -0.06 |
| Fe | 0.33 | -0.84 | 0.03 |
| Cu | 0.94 | 0.13 | -0.03 |
| Zn | 0.62 | 0.16 | 0.53 |
| Br | -0.83 | 0.11 | 0.36 |
| Rb | -0.15 | 0.17 | 0.79 |
| Sr | 0.79 | 0.45 | 0.10 |
| Zr | 0.75 | 0.37 | 0.09 |
| % of variance | 53.22 | 18.59 | 10.31 |
| Accumulative % of variance | 53.22 | 71.81 | 82.12 |

Table 2: Results of the Principal Component Analysis showing components' loadings and the % of variance explained.

Three principal components, chosen for analysis according to Guttman-Kaiser criteria (Guttman 1954; Kaiser 1960, 1970), accounted for 82.12 % of the total variance of the geochemical record (Table 2).

The first principal component (PC1) accounts for 53.22 % of the explained variance with high positive correlation coefficients for Sr, Zr, V, Mn, Cu (>0.75 p=0.05), moderate positive correlation coefficients for P, Zn, and Ti (>0.55 p=0.05), and a high negative correlation coefficient for Br (0.83 p=0.05).

The second principal component (PC2) accounts for 18.59% of the explained variance and is dominated by redox sensitive elements (S and Fe) with high negative correlation coefficients for (<-0.78, p=0.05), a moderately negative correlation coefficient for P (-0.61, p=0.05), and moderately positive correlation coefficient for Ca (0.54, p=0.05).

The third principal component (PC3) accounts for 10.31 % of the explained variance and reflects high positive correlation coefficients for K and Rb (>0.78 p=0.05), and a moderately positive correlation coefficient for Zn (0.53 p=0.05).

#### 4.2.2. PCA interpretation

*PC1*

The positively correlated elements for PC1 seem to represent, at least in part, the general, local characteristics and the natural variability of elements across the site. This group includes some elements indicative of marine environments such as Sr, V, P (Turekian 1964; Blotcki et al. 1979; Franklin 2003; Schofield et al. 2010), the origin of which might be sea spray or wave activity. Additionally, this component concentrates almost half of the variance for P, which in the case an archaeological site could suggest a contribution to this component from human activity (Holiday and Gartner 2007). A concomitant strong negative correlation for Br, a universal marine organic matter indicator (Mayer et al. 1981; Ziegler et al. 2008), complicates the interpretation. It is quite possible that the P content is a terrestrial anthropogenic component reworked by the marine environment (e.g. wave activity) and the influx of Br was due to the sea spray vector (Shotyk et al. 2003), but such a discordance between two organic matter indicators is suspicious and might indicate that the original elemental ratios were heavily distorted by diagenesis. Positive contributions of Cu, Zr, and Zn can possibly be linked with atmospheric anthropogenic pollution (Küttner et al. 2014) as a consequence of metalworking , with pollutants presumably transported and deposited by tidal and wave activity. Spatially, the PC1 raster high positive readings are concentrated over the central spot between the two structures, in the coastal area and especially in the strip on the bank of the stream channel (Fig. 3). It seems that the positive readings are somewhat related to the presence and dynamics of water. Negative readings distinguish the area west to the V-shaped structure and area on the side of the U-shaped structure. These zones interpreted as showing very little marine influence.

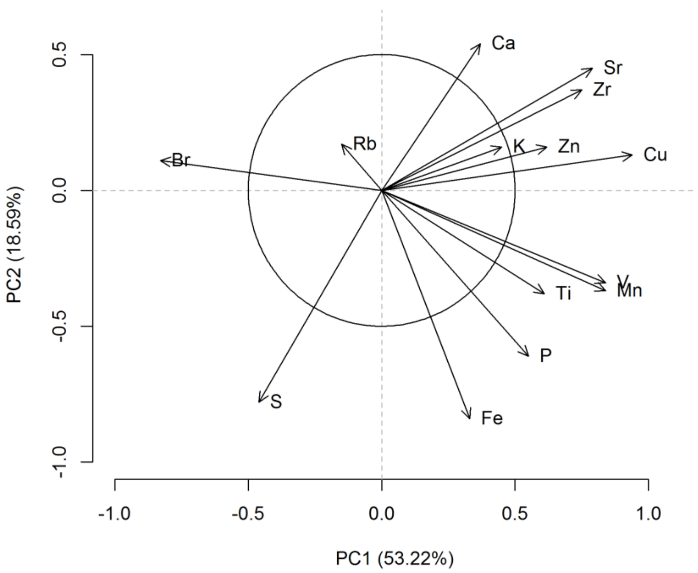


Fig. 4: Results of the Principal Component Analysis: the correlation matrix.

*PC2*

The second principal component seems to represent the biogenic contribution and is most likely to have captured any localized anthropogenic enrichment with high negative loadings from S and Fe sharing part of the P variance with PC1. This set of elements can be associated with habitation (Lutz 1951; Aston et al. 1998; Wilson 2009), the deposition of organic matter (Brady and Weil 1999, Milek and Roberts 2013; Supplement data table 3), and burning or ash deposition (Evans and Tylecote 1967; Willson et al. 2007; Milek and Roberts 2013;

Supplement data table 4). The spatial pattern of the negative readings is somewhat similar to PC1, being concentrated in a area between the structures, and also on the side and directly in front of the U-shaped building.

*PC3*

The third principal component demonstrates high positive loadings for lithogenic elements (K, Rb, Zn ) and most likely captures the results of sedimentation on site (Shotyk 1988; 2003) and presumably some disturbance through anthropogenic activities. The spatial patterning distinguishes separate zones of high positive loading between the two structures balanced by opposite readings west of the V-shaped structure and on the bank of the stream.

Most of the elements discussed here are often present in tephra (Jagan 2010; Hayward 2011). There is a tephra layer – Hekla 1693 – present in patches in the Vatnsfjörður area and it is worth to keeping in mind that even though special care was taken to sample below it, there is a possibility that due to the disturbances in stratigraphical column some of the samples might have been contaminated with ash.

## 4.3 Cluster analysis

### 4.3.1 Clustering

The composite raster consisting of three component rasters bands representing red, green and blue channels illustrates the variability of the site's elemental composition based on the PCA results. Even though there are patterns emerging that clearly separate some areas from others (e.g. the west of the V-shaped structure is distinct from the area inbetween the two structures), the boundaries remain fuzzy.  Thus, in order to efficiently divide the area of study into discrete zones, and to obtain elemental summary statistics, clustering on elemental rasters was performed (see Methodology section for details). Finally, a seven class division was chosen as the one best representing the zonation (Fig. 5). A dendrogram (Fig. 6) shows relative differences between the classes with notable affinity for classes 1, 2 and 3. Additionally, distribution of those three classes is not limited to a single location as it is characteristic for the remaining 4 classes; they are present in lcoations in the center of the sampled area. No other close grouping of classes is visible and subsequent the classes that have been distinguished are increasingly different.  Additionally, they tend to describe discrete areas on the margins of sampled area.

### 4.3.2 Class chemical composition

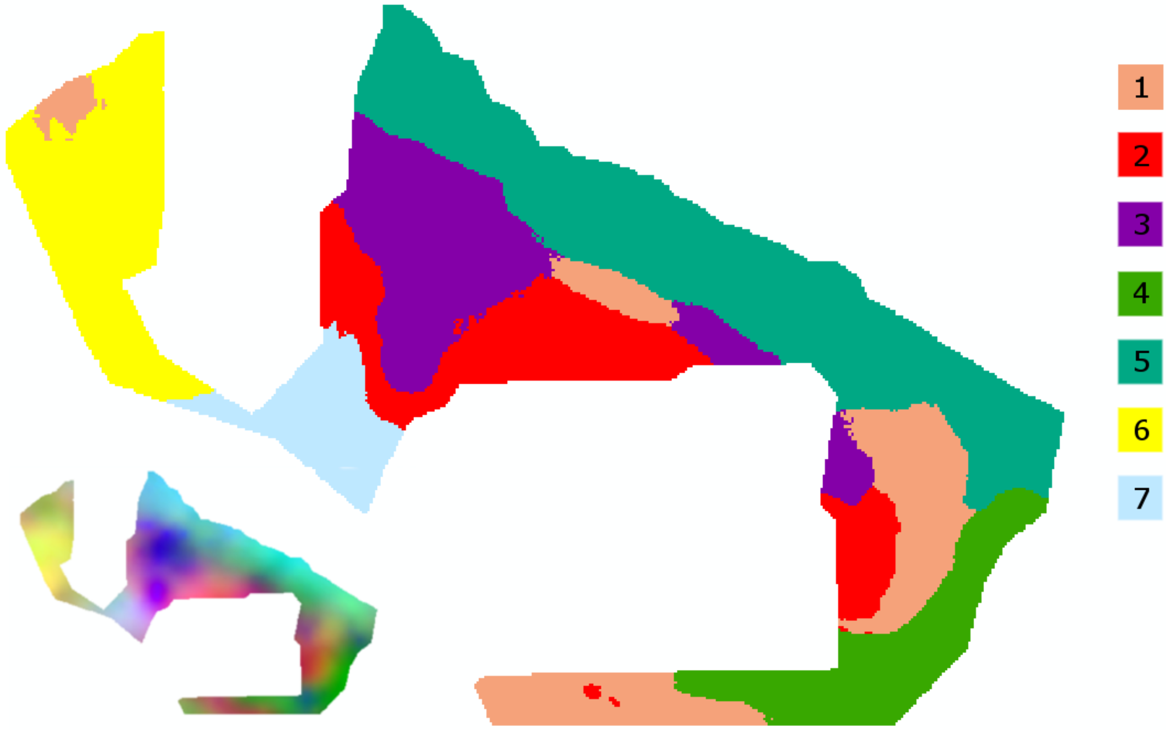


Fig. 5: Spatial distribution of the classes described in the text (the results of the Principal Component Analysis data fusion are also depicted for comparison in lower left corner of the diagram).

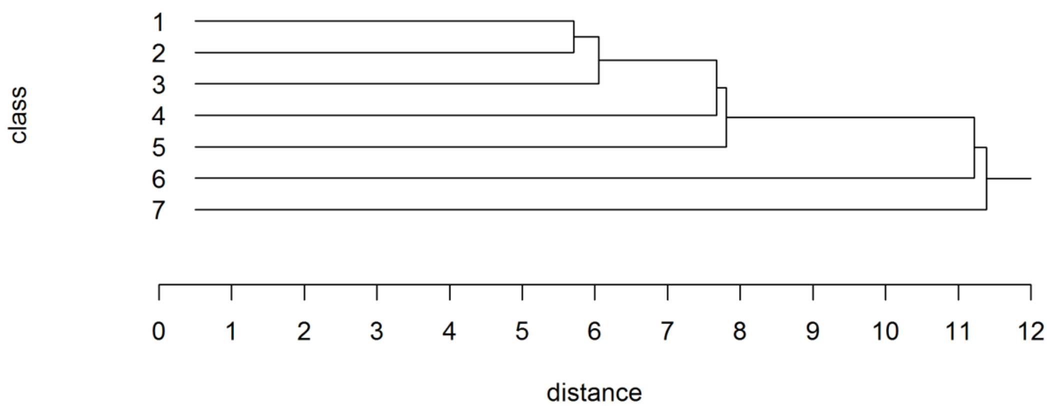


Fig. 6. Class dendrogram

Mean values of elemental readings for each class were compared with the site mean (Table 3) in order to understand the key differences between classes. Additionally, class mean values were compared with control sample means, although the first approach was favoured as a method for characterizing classes as certain doubts arose with regards to control samples being sterile from anthropogenic impact. Enrichment and depletion were specified as moderate when they differed from the mean by more than 0.5 σ and less than 1.0 σ, and strong when they differed from the mean by more than 1.0 σ.

Full consideration was given to obtaining the most reliable control groups, but the elemental readings that were produced are rather ususual (see values for C1 and C2 in Table 3). As there is uncertainty with regards to control group sterility, the interpretation presented below is based on the class comparison versus the site mean. Control values are presented for inspection only.

| vs. Site | P | S | K | Ca | Ti | V | Mn | Fe | Cu | Zn | Br | Rb | Sr | Zr |
|---|---|---|---|---|---|---|---|---|---|---|---|---|---|---|
| 1 | v | v | v | ^ | ^ | ^ | v | ^ | v | v | vv | v | v | ^ |
| 2 | v | ^^ | v | vv | v | v | v | ^ | v | vv | ^^ | v | vv | v |
| 3 | ^^^ | ^^ | ^ | ^ | ^ | ^ | ^^ | ^^^ | v | ^ | v | v | v | v |
| 4 | v | vv | v | ^^ | ^^^ | ^^^ | ^ | ^ | ^ | ^^ | vvv | vv | ^^ | ^ |
| 5 | ^ | vv | ^ | ^^ | ^ | ^ | ^ | v | ^ | ^ | v | ^ | ^^ | ^ |
| 6 | vv | v | vv | vv | vvv | vvv | vv | vvv | ^ | v | ^^ | v | v | vv |
| 7 | vv | v | ^^ | vvv | vv | vv | vv | vv | v | v | ^^^ | ^^^ | vvv | ^^ |
| C1 | vv | v | v | v | ^^ | ^^ | v | vv | v | vv | ^ | ^ | ^^ | ^ |
| C2 | v | ^ | vvv | ^^^ | ^^^ | ^^^ | ^^ | ^ | ^^^ | ^^^ | vv | vvv | ^^^ | v |

Table 3: Class elemental means (rows 1-7 , with two control groups, C1 and C2) in relation to the overall site mean. Scale runs from from strongly depleted ('vvv' in dark green) to strongly enriched ('^^^' in dark red). Signature description: $\bar{x} - \sigma/2 \leq$ 'v' $< \bar{x}$; $\bar{x} - \sigma <$ 'vv' $< \bar{x} - \sigma/2$; 'vvv' $\leq \bar{x} - \sigma$; $\bar{x} + \sigma/2 \geq$ '^' $> \bar{x}$; $\bar{x} + \sigma >$ '^^' $> \bar{x} + \sigma/2$ ; '^^^' $\geq \bar{x} + \sigma$.

The readings of P are to be treated with caution as there are reported cases of difficulties in obtaining phosphorous readings from Icelandic soils (Bolender, 2003: 42; 2006: 126; Simpson et al. 2002: 433; Mikolajczyk et al. 2015: 3). In this case, an indication that the P readings might in some way be biased is seen in the behaviour of P when measured against Br. Bromine is usually regarded as a reliable indicator of marine organic matter in a coastal environment (Mayer et al. 1981, Ziegler et al. 2008), and its behaviour should, to some degree, mimic that of P (another organic matter indicator; Olsen et al. 2015). In this case, Br is very poorly correlated with P (-0.29, p=0.05) which, in turn, is very poorly correlated with other elements usually identified as indicative of organic material (e.g. S and Sr). Conversely, the correlation with Fe is good, and it is likely that P-associated activity had little to do with accumulation of organic matter and may be linked with, for example, burning or iron-rich peat. Alternatively, Fe might indicate metalworking. It is also possible that concentrations of P were heavily distorted by post-depositional processes. Despite doubts over the precise interpretation of the P results, and because P readings appear naturally distributed, the decision was made not to exclude P from analysis as there is no clear reason to undermine the results from a methodological standpoint. The P distribution is therefore thought to reflect phenomena (not necesarly anthropogenic) that are also a part of site's history.

### 4.3.3. Class interpretation

Interpretation is based on class chemical composition as well as on their relationship to features across the site, both natural and anthropogenic (Table 4). Insofar as the class spatial distribution had a robust statistical base, the interpretation presented below is to be treated as rather speculative. There are cases where, for separate classes, similar enrichment patterns have been interpreted differently based solely on the class location within site. The background aim behind information presented in this chapter is an attempt discuss the site's historical development, devoid of any ambition to claim the undisputable.

Class 1 represents the center of the site mean. It shows a moderate depletion in Br. The indistinct character of this class suggests that it might reflect the middle ground or transition between activity zones and undisturbed terrain, or possibly a heavily-used footpath or track (Manzanilla and Barba 1990).

Class 2 shows moderate enrichment in S, Br and moderate depletion in Ca, Zn, and Sr when compared against the site mean. It represents a biogenic group of elements that is likely to be an effect of human impact. Enrichment in S and Br might indicate activities related to sea water or the use of marine equipment (Burton and Price 1990; Chagué-Goff and Fyfe 1996; Leri et al. 2010). Depletion in elements common in plant matter (Ramirez et al. 2002) might be a result of intensive wear of the grass matt and/or again indicate a heavily frequented route (Fernandez et al. 2002).

Class 3 shows strong enrichment in P and Fe as well as moderate enrichment in S and Mn. This class most likely represents the effect of intensive anthropogenic activity. The most significant characteristic of this cluster is elevated P values, presumably arising from the deposition of organic waste (Schlezinger and Howes 2000; Holiday and Gartner 2007), or (together with Fe) deposited as a result of the burning of organic matter (Willson et al. 2007), presumably Fe-rich turf. Elevated S and Mn might suggest increased microbial activity and the accumulation of decomposing organic matter (Milek and Roberts 2013; Supplement data table 3).

Class 4 shows strong enrichment in Ti and  V, moderate enrichment in Sr, Zn and Ca, strong depletion in Br, and moderate depletion in S and Rb. Both Ti and V are mobilised during the silicate weathering process and are abundant in the deposition zones of watercourses (Shiller and Mao 2000)   Sr, Zn and Ca are most likely to be linked with plant organic matter accumulation (Ramirez-Lozano et al. 2002). Br, S and Rb are often considered to be elements representative of the marine domain (Bolter et al. 1964;  Riley and Tongudai 1966; Shibagaki et al. 2008; Leri et al. 2010 ). Their absence from a marine-influenced environment might indicate this signature has been eroded by the stream.

Class 5 shows moderate depletion in S, and moderate enrichment in Ca and Sr.  Due to the sample locations, on the coastline, enrichment of thes elements is most probably reflective of a marine signature (Broecker 1970; Minoura et al. 1994; de Villiers 1999) imprinted during the prolonged process of shoreline retreat. Depletion in S is, in this case, a rather unexpected result (Casagrande et al. 1977; Chagué-Goff 2010).

Class 6 shows moderate enrichment in Br, strong depletion in V, Ti, and Fe, and moderate depletion in P, K, Ca, Mn and Zr. Enrichment in Br is most likely due to sea spray (Chen et al. 1997; Shotyk et al. 2003). General depletion in both the lithogenic and organic elements may indicate a sheltered (and unused) area,  or anthropogenic alteration possibly linked with the appearance of a depression in the ground. Recent peat cutting might explain the presence of the basin, but its influence on soil geochemistry cannot be established.

Class 7 shows strong enrichment in Br and Rb and moderate enrichment in K and Zr. It also displays strong depletion in Ca and Sr, and moderate depletion in P, Ti, V, Mn and Fe.  This class shares some similarities with Class 6 and can be interpreted as an area of low-intensity activity. Its enrichment in lithogenic elements could indicate inorganic sedimentation.

## 5. Zone interpretation and chronology in relation to RSL change-induced coastline shift

Isochrones marking significant activity episodes identified by Mikolajczyk et al. (2015) have been projected onto the map of identified activity zones for ths ite (Fig. 7). The matching of isochrones and activity zone edges was surprisingly good except for the area in the vicinity of the dry stream bed. An attempt has been made to present a spatio-chronological model of past coastal activity for this locaiton. In the event of falling RSL, an isochrone-based method can succesfuly define the timing of onset of human activity. Establishing its cessation is far more problematic due to the possible superimposition of chemical signatures from different processes. Nevertheless,  we can speculate about the date for the end of human and create a narrative of the development history for the site.

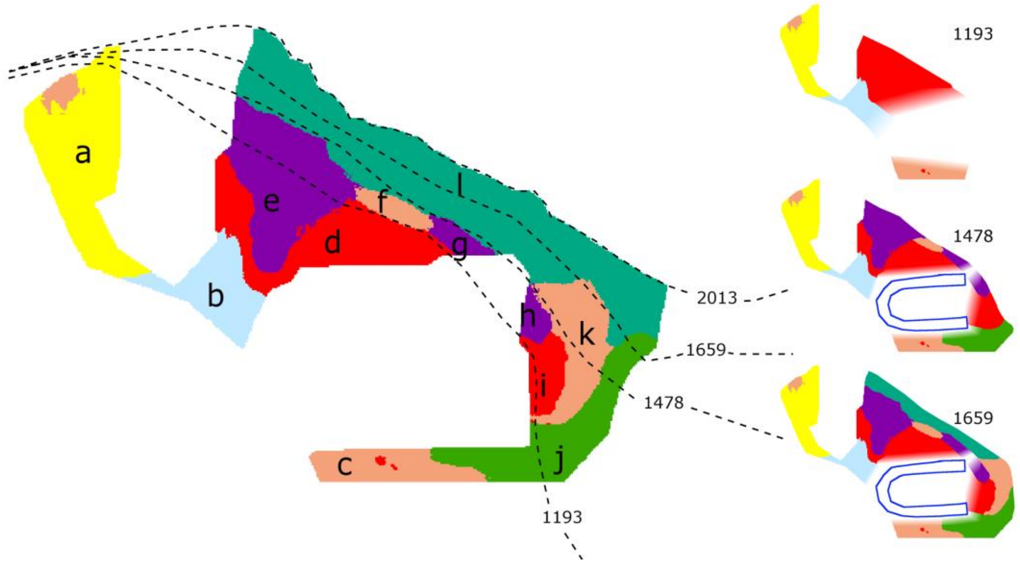


Figure 7: left: dashed lines - relative sea level isochrones linked with site activity episodes identified by Mikolajczyk et al. (2015); letters a-l - discrete activity zones. Right- suggested coastal activity development with blue polygon indicating the U-shaped structure. Shading represents missing data. Approximate dates are given in years BC.

It seems that in late 12th century, ‘d’ was the first zone active on the coast and it is quite possible that its presence was linked with the V-shaped structure. The zone’s location and its chemical character point towards it having been an area of general labour and traffic used for equipment and goods transportation.

In the late 15th century, zones ‘e’,’f’, ‘g’, ‘h’, and ‘i’ became active, probably as a consequence of falling sea level and the emergence of the U-shaped structure. Zone ‘e’ (and possibly zones of ‘g’ and ‘h’) reveal chemical signatures that suggest the deposition of organic waste material and possibly metal working. Zone ‘e’ probably overlapped with ‘d’ forming a funnel between two structures that might indicate the presence of a pathway between them. Zones ‘g’ and ‘h’ were probably connected though this relationship may be obscured by the collapse of the buildings. Zone ‘i’ carries a similar chemical fingerprint to ‘d’ and consequently may be interpreted in the same way (see above).

Zone ‘f’ is determined as having been a liminal area between activity zones and site ridges were the anthropogenic chemical signal was weaker and dispersed.

In the following period the emergence of zone ‘l’ started in the coastal area and it land it was used up until modern times. The unified chemical signature of this zone following the continuously receding coastline since the 15th century suggests that the character of this zone did not change over time. It is most likely to have been unoccupied and subject only to natural effects arising from its proximity to the marine environment.

Zone ‘k’ was probably an extension of ‘i’ and it seems to have been active until the 17th century. It’s chemical characteristics suggests similarity with zone ‘f’, a peripheral area of activity with a diluted signal.

Zone ‘j’ does not match the sea level isochrones and its extent is most likely linked with the dynamics of the stream. Its emergence might have started together with the earliest activity recorded on site, and its development was most likely interrupted in the 17th century due to the disappearance of the stream.

In terms of chronology, location in relation to structures might generally indicate an earlier date for ‘a’ and ‘b’ and a later date for ‘c’. Despite being close to the shoreline, zone ‘a’ scores negatively in the marine-influenced principal component (PC1). This may indicate anthropogenic alteration with peat cutting seeming the most reasonable possibility.

Zone ‘b’ has a chemical signature indicating inorganic sedimentation and it correlates with the area that appeared different during sampling as the sediment seemed to be mixed with structural collapse. It is therefore possible that the area’s original signature was mixed with the leveled material from the nearby building.

Zone ‘c’ carries a signature similar to the ones interpreted as general working areas. It is likely that it formed a work space linked with the U-shaped structure. Unfortunately this zone lies on the edge of sampled area and the full extent of this unit cannot be traced.

| Zone | Class | Class interpretation | elevated elements | depleted elements | chemical signature dating |
|---|---|---|---|---|---|
| a | 6 | sheltered area, peat cutting | Br | V, Ti, Fe P, K, Ca, Mn, Zr | n/a |
| b | 7 | mixed, structure collapse | Br, Rb, K, Zr | Ca, Sr, P, Ti, V, Mn, Fe | n/a |
| c | 1 | edge of activity zone | n/a | Br | n/a |
| d | 2 | general labour, traffic | S, Br | Ca, Zn, Sr | ante 1193 |
| e | 3 | o.m. deposition, burning, metalworking | P, Fe, S, Mn | n/a | 1193 |
| f | 1 | edge of activity zone | n/a | Br | 1193 - (1478) |
| g | 3 | o.m. deposition, burning, metalworking | P, Fe, S, Mn | n/a | 1193 - (1478) |
| h | 3 | o.m. deposition, burning, metalworking | P, Fe, S, Mn | n/a | 1193 - (1478) |
| i | 2 | general labour, traffic | S, Br | Ca, Zn, Sr | 1193 - (1478) |

| | | | | | |
|---|---|---|---|---|---|
| j | 4 | stream bed, natural | Ti, V, Sr, Zn and Ca | Br, S, Rb | n/a |
| k | 1 | edge of activiti zone | n/a | Br | 1478 – (1659) |
| l | 5 | shoreline, natural | Ca, Sr | S, | 1478 - 2013 |

Table 4. Zone characteristics; class affiliation, functional interpretation, chemical properties and relative sea level-based dating (in brackets are the presumed activity cessation dates).

## 6. Conclusions

This study has proven successful in applying a multi-elemental dataset to characterise the use of archaeological space on the coast at Vatnsfjörður. The approach can be viewed as an alternative to standard excavation with modest test-pit sampling. The method gives insight into the key factors that shaped local geochemistry and has allowed informed distinctions to be made between anthropogenic pressure and natural processes. We have speculated about the functional use of space across the site and the site's chronology through its relationship to RSL-induced coastal shift. There is plenty of room to further develop the method to incorporate proxies beyond the geochemical suite of elements presented here (e.g. through assessment of biomolecules like proteins, lipids or carbohydrates). This may provide further information about particular activities performed on the site.

## 7. Acknowledgements

The research was funded through a scholarship awarded by the University of Aberdeen's FAR North programme, and by the Carnegie Trust for the Universities of Scotland. We are very grateful to FornleifastofnunIslands and the crew of the 2013 field school at Vatnsfjorður for their support with fieldwork, especially Oskar Gísli Sveinbjarnarson, Dawn Elise Mooney and Garðar Guðmundsson. We would also like to express our gratitude to James Parker, Kayleihg Hamilton and OLYMPUS Corporation for providing the 'Olympus-Innov-X Delta Premium XRF' scanner. We are indebted to Edward Schoffield for proof-reading and editting the manuscript. We would also like to thank two anonymous rewievers for their insightful comments.

## 8. References

Arnalds, O. (2004). Volcanic soils of Iceland. Catena, 56, 3-10.

Arnalds, O., Hallmark, C.T., Wilding, L.P. (1995). Andisols from four different regions of Iceland. Soil Science Sociology American Journal, 59, 161-169.

Aston, M.A., Martin, M.H., Jackson, A.W. (1998). The use of heavy metal soil analysis for archaeological surveying, Chemosphere, 37, 3, 465-477.

Baxter, M.J. (1995). Standardization and Transformation in Principal Component Analysis, with Applications to Archaeometry. Applied Statistics-Journal of the Royal Statistical  Society Series C. Applied Statistics-Journal of the Royal Statistical Society Series C, 44 ,4, 513-527.

Blotcky A.J., Falcone, C., Medina, V.A., Rack, E.P., Hobson, D.W. (1979). Determination of trace-level vanadium in marine biological samples by chemical neutron activation analysis. Analytical Chemistry, 51, 178–182.

Bolender, D. J. (2006). The Creation of a Propertied Landscape: Land Tenure and Agricultural Investment in Medieval Iceland (unpublished PhD thesis). Northwestern University.

Bolter, E., Turekian, K. K.,  Schutz, D. F., (1964).The distribution of rubidium, cesium and barium in the oceans, Geochimica et Cosmochimica Acta, 28, 9, 1459-1466.

Brady, N. C., Weil, R. R. (1999). The nature and properties of soils.

Burton, J.H.,Price, T.D. (1990). The ratio of barium to strontium as a paleodietary indicator of consumption of marine resources. Journal of Archaeological Science, 17, 547-557.

Casagrande, D. J. ,  Siefert, K.  Berschinski, C., Sutton,N. (1977) Sulfur in peat-forming systems of the Okefenokee Swamp and Florida Everglades: origins of sulfur in coal, Geochimica et Cosmochimica Acta, 41, 161-167.

Chagué-Goff, C. (2010). Chemical signatures of palaeotsunamis: A forgotten proxy?, Marine Geology, 271, 67-71.

Chagué-Goff, C.,  Fyfe, W.S. (1996)Geochemical and petrographical characteristics of a domed bog, Nova Scotia: a modern analogue for temperate coal deposits, Organic Geochemistry, 24, 141–15.

Chambers, R. L., Kokic, P., Smith, P., Cruddas, M. (2000). Winsorization for identifying and treating outliers in business surveys. Proceedings of the 2nd International Conference on Establishment Surveys. Statistics Canada. Ottawa, Canada, 717-726.

Z. Chen, Z. Chen, W. Zhang  (1997)Quaternary stratigraphy and trace-element indices of the Yangtze Delta, Eastern China, with special reference to marine transgressions. Quaternary Research, 47, 181–191

Craig, N., Aldenderfer, M., & Moyes, H. (2006). Multivariate visualization and analysis of photomapped artifact scatters. Journal of Archaeological Science, 33, 1617–1627.

Devereux, B. J., Amable, G. S., & Crow, P. (2008). Visualisation of LiDAR terrain models for archaeological feature detection. Antiquity, 82, 470–479.

Dore, C. D., López Varela, S. L.  (2010) Kaleidoscopes, Palimpsests, and Clay: Realities and Complexities in Human Activities and Soil Chemical/Residue Analysis. Journal of Archaeological Method and Theory, 17, 279-302.

Entwistle, J.A., McCaffrey, K.J.W., Dodgshon, R.A. (2007) Geostatistical and multi-elemental analysis of soils to interpret land-use history in the Hebrides, Scotland. Geoarchaeology, 22, 4, 391-415.

ESRI (2015). ArcGIS Desktop: Release 10. Redlands, CA: Environmental Systems Research Institute.

Evans, R.T. and Tylecote, R.F., (1967). Some vitrified products of non-metallurgical significance. Bulletin of the Historical Metallurgy Group ,8, 22-23.

Fernandez, F.G., Terry, R.E., Inomata, T., Eberl, M. (2002). An ethnoarchaeological study of chemical residues in the floors and soils of Q'eqchi' Maya houses at Las Pozas, Guatemala. Geoarchaeology, 17, 487–519.

Franklin, J. N. (2003). The Role of Vanadium Bromoperoxidase in the Biosynthesis of Halogenated Marine Natural Products. Unpublished PhD Thesis, University of California, Santa Barbara.

Guttman, L. (1954). Some necessary conditions for common factor analysis. Psychometrika, 19, 149–161.

Hayward, C. (2012). High spatial resolution electron probe microanalysis of tephras and melt inclusions without beam-induced chemical modification. Holocene, 22, 1, 119-125. Holliday, V.T., Gartner, W.G. (2007). Methods of soil P analysis in archaeology. Journal of Archaeological Science, 34, 301-333.

Holliday, V. T., Gartner, W. G. (2007). Methods of soil P analysis in archaeology. Journal of Archaeological Science, 34, 301-333

Hotelling, H. (1933). Analysis of a complex of statistical variables into principal components. Journal of Educational Psychology, 24, 417–441.

Ilves, K., Darmark, K. (2011). Some Critical and Methodological Aspects of Shoreline Determination: Examples from the Baltic Sea Region. Journal of Archaeological Method and Theory, 18, 147-165.

Jagan , A., (2010). Tephra stratigraphy and geochemistry from three Icelandic lake cores: a new method for determining source volcano of tepra layers university of Edinburgh.

Kaiser, H.F. (1960). The application of electronic computers to factor analysis. Educational and Psychological Measurement, 20, 141–151.

Kaiser, H.F. (1970). A second generation Little Jiffy. Psychometrika, 35 ,401–417.

Knudson, K. J., Frink, L., Hoffman, B. W., & Price, T. D. (2004). Chemical characterization of Arctic soils: Activity area analysis in contemporary Yup'ik fish camps using ICP-AES. Journal of Archaeological Science, 31, 8, 443-456.

Küttner, A., Mighall, T. M., De Vleeschouwer, F., Mauquoy, D., Martínez Cortizas, A., Foster, I. D .L., Krupp, E. (2014). A 3300-year atmospheric metal contamination record from Raeburn Flow raised bog, south west Scotland, Journal of Archaeological Science,44, 1-11.

Kvamme, K. L. (2006). Integrating multidimensional geophysical data. Archaeological Prospection, 13, 1, 57–72.

Kvamme, K. L. (2007). Integrating multiple geophysical datasets. In Wiseman, J., El-Baz, F. (Eds.),Remote sensing in archaeology, New York, Springer, 345–374.

Leri, A., Hakala, J., Marcus, M., Lanzirotti, A., Reddy, C., Myneni, S. (2010). Natural organobromine in marine sediments: New evidence of biogeochemical Br cycling. Global Biogeochemical Cycles, 24.

Linderholm, J., Lundberg, E. (1994). Chemical Characterization of Various Archaeological Soil Samples using Main and Trace Elements determined by Inductively Coupled Plasma Atomic Emission Spectrometry. Journal of Archaeological Science, 21, 3, 303-314.

Lloyd, J.M., Dickens, W. (2011). Relative sea-level change and coastal evolution from Sveinhúsavatn, Vatnsfj€orður, NW Iceland. Unpublished report for Fornleifastofnun Islands.

Lutz, H. J. (1951) Concentration of Certain Chemical Elements in the Soils of Alaskan Archaeological Sites. American Journal of Science. 249, 12, 925-928.

Manzanilla, L., Barba, L. (1990). The Study of Activities in Classic Households: Two Case Studies from Coba and Teotihuacan. Ancient Mesoamerica, 1, pp 41-49

Mayer, L. M., Macko, S. A., Mook, W. H., Murray, S. (1981). The distribution of bromine in coastal sediments and its use as a source indicator for organic matter. Organic Geochemistry, 3, 37-42.

Middleton, W. D., Price, T. D. (1996) (with) Chemical Analysis of Modern and Archaeological House Floors by Inductively Coupled Plasma- Atomic Emission Spectroscopy. Journal of Archaeological Science 23 (5): 673-687.

Middleton W. D., Barba L., Pecci A., Burton J.H, Ortiz A., Salvini L., Rodriguez Suárez R. (2010). The Study of Archaeological Floors: Methodological Proposal for the Analysis of Anthropogenic Residues by Spot Tests, ICP-OES, and GC-MS. Journal of Archaeological Method and Theory, 17, 183-208.

Mikołajczyk, Ł. (2013). Chemical properties of possible floor deposit [12026] from structure 5 (Area 45, VSF12). In: Isaksen, O. (Ed.), Vatnsfj€orður 2012: Framvinduskýrslur/Interim Report. Fornleifastofnun Islands, Reykjavík, pp. 56E60. Available from: http://www.instarch.is/pdf/uppgraftarskyrslur/FS514-030912_Vatnsfj%C3%B6r%C3%B0ur%202012.pdf (12.04.16.).

Mikołajczyk, Ł., Gardeła, L. (2010). GPS survey in the coastal area of Vatnsfj€orður. In: Milek, K. (Ed.), Vatnsfj€orður 2009: Framvinduskyrslur/Interim Report. Fornleifastofnun Islands, Reykjavík, pp. 41-50. Available from: http://www.instarch.is/pdf/uppgraftarskyrslur/FS449-03099_Vatnsfj%C3%B6r%C3%B0ur%202009.pdf (19.04.16.).

Mikołajczyk, Ł., Ilves, K., May, J., Sveinbjarnarson, O., Milek, K. (2015). Use of phosphorus mapping in assessing coastal activity zones of an Icelandic multi-period site of Vatnsfjörður, Journal of Archaeological Science, 59, 1-9.

Milek, K. (2011). Samantekt/Overview. In: Milek, K. (Ed.), Vatnsfj€orður 2010: Framvinduskýrslur/Interim Report. Fornleifastofnun Islands, Reykjavík, 15-24. Available from: http://www.instarch.is/pdf/uppgraftarskyrslur/FS461-030910%20Vatnsfj%C3%B6r%C3%B0ur%202010%20Interim%20Reports.pdf (10.05.16.).

Milek, K. B., Roberts, H. M. (2013). Integrated geoarchaeological methods for the determination of site activity areas: A study of a Viking Age house in Reykjavik, Iceland. Journal of Archaeological Science, 40, 4, 1845-1865.

Minoura, K., Nakaya, S., Uchida, M. (1994). Tsunami deposits in a lacustrine sequence of the Sanriku coast, northeast Japan, Sedimentary Geology, 89, 25–31.

Misarti, N., Finney B., and Maschner H. (2011). Reconstructing site organization in the eastern Aleutian Islands, AK using multi-element chemical analysis of soils. Journal of Archaeological Science 38, 7, 1441-1455.

Mooney, D.E. (2011). Evaluation trenches excavated at vatnsfj€orður. In: Milek, K. (Ed.), Vatnsfj€orður 2010: Framvinduskýrslur/Interim Report. Fornleifastofnun Islands, Reykjavík, pp. 69e75. http://www.instarch.is/pdf/uppgraftarskyrslur/FS461-030910%20Vatnsf%C3%B6r%C3%B0ur%202010%20Interim%20Reports.pdf (06.05.16.).

Mooney, D.E., Sveinbjarnarson, O.G., Mikołajczyk, Ł. (2012). Evaluation trenches and Excavations of the coastal structures at vatnsfj€orður. In: Isaksen, O. (Ed.), Vatnsfj€orður 2011: Framvinduskýrslur/Interim Report. Fornleifastofnun Islands, Reykjavík, pp. 47e64. Available from: http://www.instarch.is/pdf/uppgraftarskyrslur/FS492-030911_Vatnsfj%C3%B6r%C3%B0ur%202011.pdf (08.05.16.).

Mooney, D.E. (2013). Excavations of the Costal structures at vatnsfj€orður: areas 45 & 46. In: Isaksen, O. (Ed.), Vatnsfj€orður 2012: Framvinduskýrslur/Interim Report. Fornleifastofnun Islands, Reykjavík, pp. 40e55. Available from: http://www.instarch.is/pdf/uppgraftarskyrslur/FS514-030912_Vatnsfj%C3%B6r%C3%B0ur%202012.pdf (08.05.16.).

Norðdahl, H., Petursson, H.G. (2005). Relative sea-level changes in Iceland; new aspects of the Weichselian Deglaciation of Iceland. In: Caseldine, C., Russel, A., Hardardottir, J., Knudsen, O. (Eds.), Iceland e Modern Processes and Past Environments, 25-78.

Olsen, D. J. R., Endelman, J. B., Jacobson, A. R., Reeve, J. R. (2015). Compost Carryover: Nitrogen Phosphorous and FT-IR Analysis of Soil Organic Matter . Plants, Soils, and Climate Faculty Publications. Paper 733.

Oonk S., Slomp, C. P., Huisman, J. D. (2009). Geochemistry as an aid in archaeological prospection and site interpretation: current issues and research directions. Archaeological Prospection, 16, 35–51.

Pearson, K., (1901) On lines and planes of closest fit to systems of points in space. Philosophical Magazine, Series 6, 2, 559–572.

R Core Team. (2014). R: A language and environment for statistical computing. R Foundation for Statistical Computing, Vienna, Austria.

Ramirez L., Roque, G., Humberto, G. R., Guillermo, G. D. (2002). Chemical composition and rumen digestion of foragefrom kleingrass (panicum coloratum). INCI , 27, 12, 705-709.

Richards, J. A., & Jia, X. (1999). Remote sensing digital image analysis: An introduction. New York: Springer.

Schiller, A.M., Mao, L. (2000). Dissolved V in rivers: effects of silicate weathering. Chemical Geology, 165, 13–22.

Schlezinger, D.R. and B.L. Howes. (2000). Organic phosphorus and elemental ratios as indicators of prehistoric human occupation. Journal of Archaeological Science , 27, 479-492.

Schofield, J. E., Edwards, K. J., Mighall, T. M., Martínez Cortizas, A., Rodríguez-Racedo, J., Cook, G. (2010) An integrated geochemical and palynological study of human impacts, soil erosion and storminess from southern Greenland since c. AD 1000. Palaeogeography, Palaeoclimatology, Palaeoecology, 295, 19–30.

Shibagaki, N., Pootakham, W., Grossman, A. R. (2008). The responses of algae to their sulfur environment. In Advances in Photosynthesis and Respiration. Hell, R. Dahl, C., Knaff, D., Leustek, T. (Eds). Invited Review, 231-267.

Shotyk, W. (1988). Review of the inorganic geochemistry of peats and peatland waters. Earth-Science Reviews, 25, 95–176.

Simpson, I.A., Adderley, W.P., Guðmundsson, G., Hallsdottir, M., Sigurgeirsson, M.A., Snæsdottir, M. (2002). Soil limitations to agrarian land production in premodern Iceland. Human Ecology, 30, 4, 423-443.

de Villiers S. (1999) Seawater strontium and Sr/Ca variability in the Atlantic and Pacific oceans. Earth and Planetary Science Letters 171, 623-634.

Turekian K. K. (1964). The marine geochemistry of strontium. Geochimica et Cosmochimica Acta, 28, 1479–1496.

Wilson, C.A., Davidson, D.A., Cresser, M.S. (2007). Evaluating the use of multi-element soil analysis in archaeology: a study of a post-medieval croft (Olligarth) in Shetland. Atti della Società Toscana di Scienze Naturali 112, 69–78.

Wilson,C. A., Davidson, D. A., Cresser, M.S. (2009). An evaluation of the site specificity of soil elemental signatures for identifying and interpreting former functional areas, Journal of Archaeological Science, 36, 10, 2327-2334.

Ziegler, M., Jilbert, T., de Lange, G. J., Lourens, L. J., Reichart, G. J. (2008). Bromine counts from XRF scanning as an estimate of the marine organic carbon content of sediment cores. Geochemistry, Geophysics, Geosystems, 9, 1525-2027.